Materials Science & Engineering A 670 (2016) 153–158

Contents lists available at ScienceDirect

Materials Science & Engineering A

journal homepage: www.elsevier.com/locate/msea

Enhanced mechanical properties of medium carbon steel casting via friction stir processing and subsequent annealing

P. Xue [a], W.D. Li [a,b], D. Wang [a], W.G. Wang [a], B.L. Xiao [a], Z.Y. Ma [a,*]

[a] Shenyang National Laboratory for Materials Science, Institute of Metal Research, Chinese Academy of Sciences, 72 Wenhua Road, Shenyang 110016, China
[b] Kocel Group Limited, 199 South Tongxin Street, Yinchuan 750021, China

ARTICLE INFO

Article history:
Received 12 February 2016
Received in revised form
6 June 2016
Accepted 8 June 2016
Available online 9 June 2016

Keywords:
Friction stir processing
Ultrafine-grained structure
Medium carbon steel
Microstructure
Mechanical property

ABSTRACT

This study provides an effective surface processing technology to increase the local mechanical properties of medium carbon steel castings. Ultrafine dual-phase structure of the ferrite and the martensite was obtained in the processed zone with a depth of 1 mm via submerged friction stir processing (FSP). Significantly enhanced yield strength (YS) of 2070 MPa was achieved in the FSP steel compared to that of the base material (BM) with a relatively low YS of 590 MPa, but a low uniform elongation (UE) of 3.0% was achieved compared to that of the BM (9.4%). After annealing, obvious carbide precipitation was observed in the original quenched martensite phases. Therefore, good strength-ductility synergies with high YS of 1020 MPa and 925 MPa, and acceptable UE of 5.9% and 9.3% were achieved in the FSP steel after annealed for 2 h at 500 °C and 600 °C, respectively.

1. Introduction

Medium carbon steel castings are widely used in mining machinery, and high hardness, high strength and certain toughness are generally required for these castings [1,2]. Therefore, various heat treatment methods, such as quenching, normalizing and annealing are applied to increase the mechanical properties of the castings [3]. However, for the large machinery castings, a low cooling rate is often achieved in local regions, resulting in lower strength and hardness in these regions compared to the whole castings.

It is noted that higher hardness and strength may be required only in some specific parts of the castings, such as the surface. Increasing the contents of the alloy elements to increase the carbon equivalent (Ceq) and improving the heat treatment condition on the whole casting can meet the local mechanical property requirement [1,3]. However, this would lead to increased cost. Therefore, seeking for other low-cost methods to improve the local mechanical properties of the steel castings is highly desired.

Besides changing the chemical composition and heat treatment condition, various surface severe plastic deformation (SPD) methods, such as shot peening (SP) [4,5], surface mechanical attrition treatment (SMAT) [6,7] and friction stir processing (FSP) [8,9] provide feasible solutions to improving the local mechanical properties of the large castings. Among these methods, FSP is an effective thermo-mechanical processing technology, developed based on the principles of the friction stir welding (FSW) [8–10]. FSP causes significant microstructural refinement, densification, and homogeneity of the processed zone (PZ), thereby improving the properties of the materials. It has been demonstrated that enhanced hardness, strength, fatigue limit, wear and erosion resistance can be obtained in various steels after FSP [9,11–14].

Similar to other SPD methods, FSP is also effective in preparing ultrafine-grained (UFG) structure in the surface layer of the metallic components [15–19]. More importantly, much larger processing depth can be achieved compared to other SPD methods. Xue et al. [20] reported that an obvious PZ with a depth of 2 mm could be obtained even using the FSP tool without pin. Besides, various ultrafine transformed phase structures can be obtained in carbon steels via FSP, resulting in excellent mechanical properties [12,14,20]. It was reported that ultrahigh ultimate tensile strength (UTS) of 1.3 GPa together with a uniform elongation (UE) of 7% were achieved in a plain low carbon steel after FSP, which consisted of ultrafine ferrite and martensite phases [20]. Therefore, FSP should be an optimal solution for improving the local mechanical properties of large medium carbon steel castings.

However, the investigations on FSP of steels are still limited due to the processing inconvenience and the complex phase transformation [21,22]. Therefore, further investigations on FSP of steels are still needed to understand the microstructural evolution and its effect on the mechanical properties of the FSP steels.

* Corresponding author.
E-mail address: zyma@imr.ac.cn (Z.Y. Ma).

http://dx.doi.org/10.1016/j.msea.2016.06.014
0921-5093/

In the present study, submerged FSP was performed on a medium carbon steel casting with rapid water cooling, and subsequent annealing was applied to improve the ductility and the toughness. The aim of this study is to investigate whether improved mechanical properties can be achieved on the local surface of the casting and to elucidate the microstructure-property correlation in the FSP medium carbon steel.

2. Experimental procedures

The materials used in this study were 6 mm thick medium carbon steel plates machined from the attached castings during the production of the cone crusher, which is a typical large machinery casting in Kocel Group Limited, and the chemical composition of the steel is shown in Table 1. The carbon equivalent (Ceq) was about 0.64 calculated by the following equation [23]:

$$Ceq=C + Mn/6 + (Cr+Mo + V)/5 + (Ni + Cu)/15 \quad (1)$$

In order to improve the mechanical properties, the base material (BM) was first held at 920 °C for 12 h, and then quenched by strong wind at a cooling rate of about 20 °C min^{-1}. Finally, the BM was annealed at 620 °C for 12 h to improve the ductility and the toughness, and the mechanical properties of the BM are shown in Table 2.

Submerged FSP was conducted at a low heat input with a tool rotation rate of 400 rpm and a traverse speed of 50 mm min^{-1}. A tool with a shoulder 10 mm in diameter without stirring pin was used, and the whole tool was made of the common tool steel whereas the end of shoulder part that was made of TiC-based cermet. In order to obtain a very low heat input and a rapid cooling rate, the steel plates were first fixed in water and additional rapid cooling with flowing water was used during the FSP process. Detailed parameters about the water cooling have been stated in the previous study [24]. In order to improve the ductility and the toughness, the FSP samples were annealed for 2 h at 500 and 600 °C, respectively.

Microstructural characterization and analysis were carried out by the optical microscopy (OM) and the scanning electron microscopy (SEM). The samples were cross-sectioned perpendicular to the processing direction, polished and then etched in 5% nital for 5 s. The microstructure observation was performed on Leica DMI 5000M OM and FEI Quanta 600 SEM.

The Vickers microhardness test was performed on Akashi MVK-H300 microhardness tester using 1000 g load for 10 s. Tensile specimens of 5 mm gauge length, 1.2 mm gauge width and 0.6 mm gauge thickness were machined from the PZ perpendicular to the FSP direction. Meanwhile, tensile specimens with the same dimensions were machined from the BM. The tensile tests were carried out on Instron 5848 microtester at an initial strain rate of 1×10^{-3} s^{-1}.

3. Results and discussion

Fig. 1 shows the cross-sectional macrograph of the FSP medium carbon steel sample. An obvious PZ could be observed though no stirring pin was used. The width of the PZ was 10 mm and comparable to the shoulder diameter, attributed to the effect of the shoulder. Furthermore, the depth of the PZ was 1.5 mm, which is much larger than that obtained by the SP or SMAT technique [4–7]. Similar to the FSP low carbon steel, relatively uniform microstructure was achieved in the upper part of the PZ with a depth of about 1 mm [20].

The initial BM exhibited a typical microstructure of the large castings after the heat treatment, which was composed of coarse ferrite and bainite phases, as shown in Fig. 2(a). The ferrite phases exhibited polygonal grains with a wide size range from several to several tens of micrometers, and coarse bainite phases as large as hundreds of micrometers were observed in the BM. However, the grains were significantly refined in the PZ after FSP (Fig. 2(b)), and it was difficult to discern the exact microstructure from the OM image.

Fig. 3 shows the detailed SEM microstructure of the BM and the PZ. It is clear that lots of carbide particles were distributed along the bainite laths in the BM (Fig. 3(a)), which exhibited obvious tempered microstructure. Nearly equiaxed grains were obtained in the PZ after FSP, and a typical ultrafine dual-phase structure of ferrite and martensite phases could be observed, as shown in Fig. 3 (b). The grain size of the ferrite phase was about 1–2 μm, and the martensite phase showed slightly larger size. Different from the FSP low carbon steel [20], the microstructure of the FSP medium carbon steel was in quenched state, and the carbide particles were hardly observed (Fig. 3(b)), which is attributed to the high Ceq (~0.64) of the medium carbon steel used in this study.

Obviously, the phase transformation occurred during FSP of the medium carbon steel, indicating that the processing temperature was higher than Ac_1. According to the previous studies together with the microstructural characteristics, the temperature was greatly reduced due to the rapid water cooling, and the maximum processing temperature should be lower than Ac_3, i.e., within a $(\gamma+\alpha)$ 2-phase field [3,15–20]. Therefore, during the FSP process, part of the original ferrite phase (including bainite) transformed to the austenite phase, and then transformed to the martensite phase during the subsequent rapid water cooling. Furthermore, dynamic recrystallization of the ferrite and the austenite phases occurred during the FSP process due to the intense plastic deformation, resulting in the ultrafine structure [11–15]. Meanwhile, the original carbides in the bainite phases were dissolved due to the high temperature and severe plastic deformation during FSP, and the carbon atoms diffused into the austensite matrix. In this case, ultrafine dual-phase structure of the ferrite and the martensite phases was achieved, but the characteristic of the martensite phase was not obvious due to its quenched state.

Fig. 4 shows the hardness distributions in the cross-section along the horizontal and longitudinal lines, respectively. The BM exhibited a relatively low hardness value of ~240 Hv. By comparison, much higher hardness value of ~650 Hv was obtained in the PZ of the FSP steel (Table 2). Furthermore, relatively

Table 2
Hardness and tensile properties of the base material and FSP steel.

Samples	Hardness (Hv)	YS (MPa)	UTS (MPa)	UE (%)	El. (%)
BM	240	590	840	9.4	21.8
FSP	650	2070	2405	3.0	4.0
FSP-500	438	1270	1320	5.9	18.8
FSP-600	337	925	1020	9.3	23.4

Table 1
Chemical composition of the base material (in wt%).

Element	C	Si	Mn	P	S	Ni	Cr	Mo	Cu	Fe
Content	0.289	0.64	1.613	0.014	0.004	0.214	0.241	0.094	0.041	Bal.

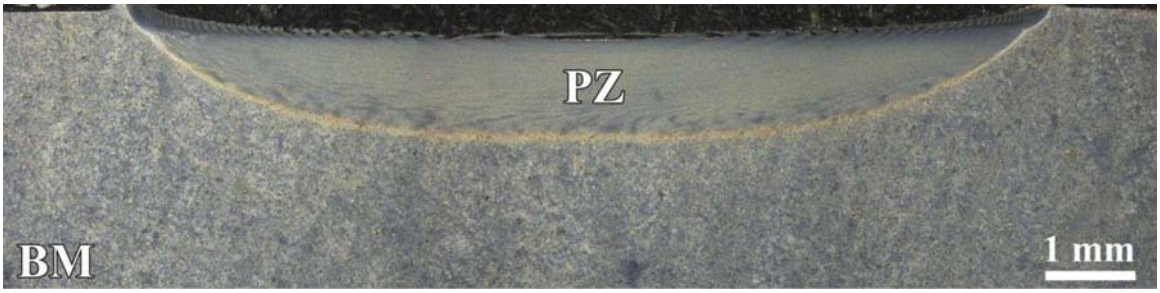

Fig. 1. Macrostructure of FSP medium carbon steel.

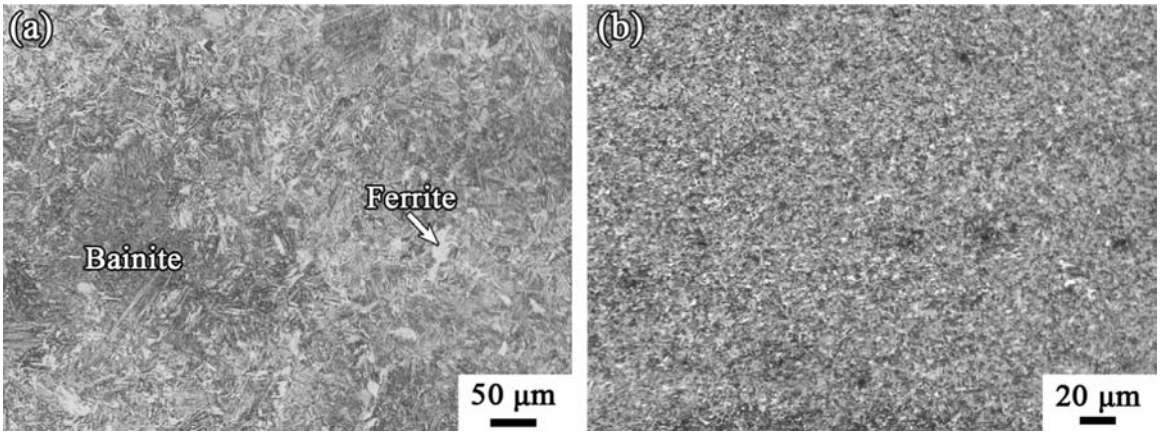

Fig. 2. Microstructure of (a) BM and (b) PZ of FSP steel.

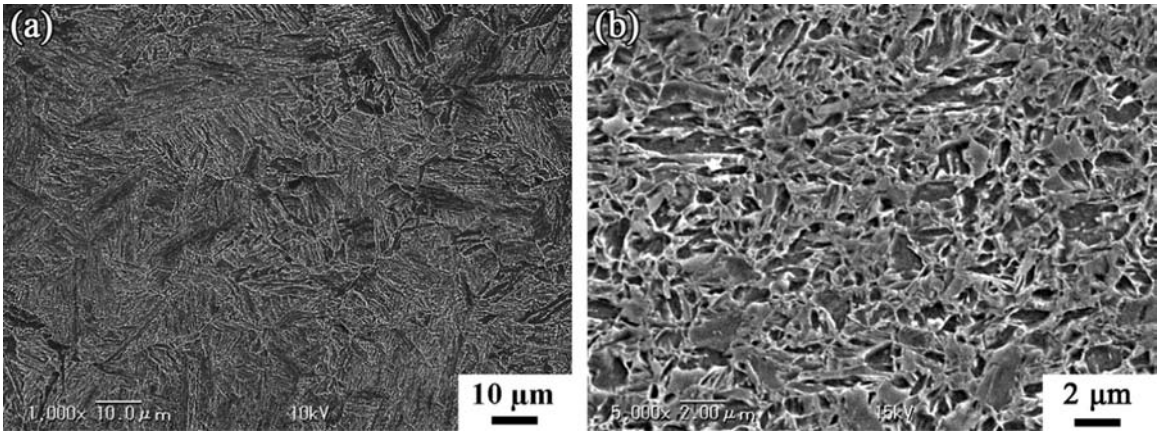

Fig. 3. SEM microstructure of (a) BM and (b) PZ of FSP steel.

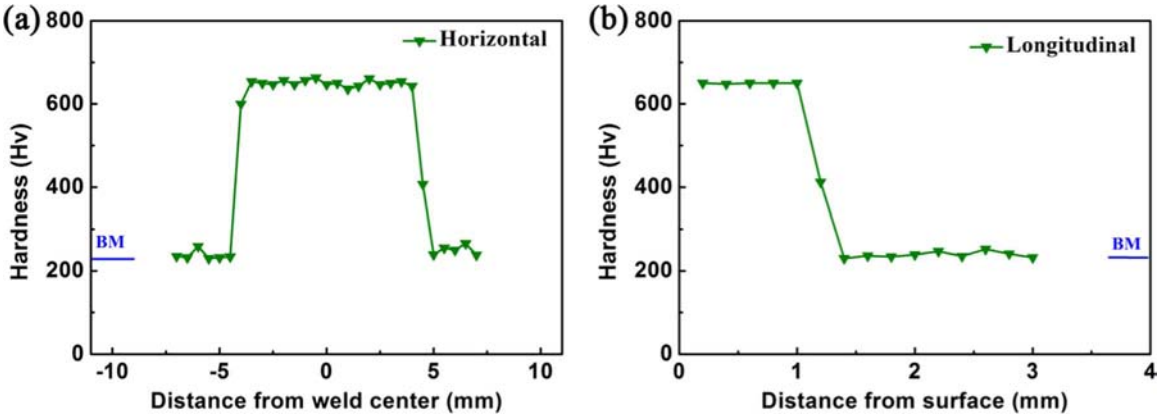

Fig. 4. Hardness distributions along (a) horizontal and (b) longitudinal lines on cross-section of FSP steel.

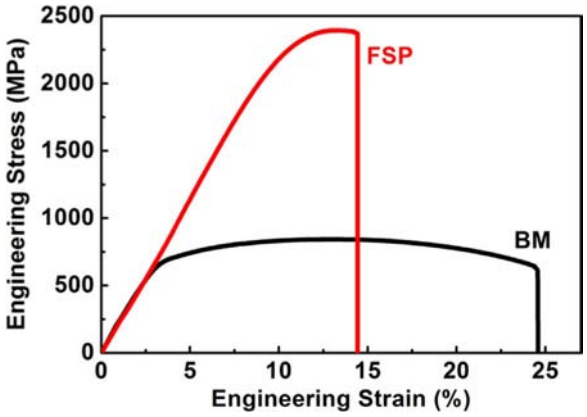

Fig. 5. Engineering stress-strain curves of BM and FSP steel.

homogeneous hardness distributions were observed in the PZ along both the horizontal and longitudinal lines. Meanwhile, the depth of the high hardness zone was larger than 1 mm in the PZ, which means that, a uniform PZ with much larger depth than that obtained by other SPD methods was obtained in the FSP medium carbon steel.

Fig. 5 shows the typical tensile curves of the BM and the FSP samples, and the related results are summarized in Table 2. The yield strength (YS) and UTS of the BM were about 590 and 840 MPa, and the UE and total elongation were about 9.4% and 21.8%, respectively. After FSP, very high YS of 2070 MPa and UTS of 2405 MPa were obtained in the PZ. However, the elongation sharply decreased to about 4.0%, and the UE was only 3.0%, which was lower than the utilizable UE in industrial application (5%).

Compared to the BM, the tensile ductility clearly decreased in the FSP medium carbon steel, though very high strength was achieved. Moreover, the elongation was also lower than that of the FSP low carbon steel with an UE of 7%, though similar FSP parameters were used [20]. This should be related to the enhanced quenching tendency in the medium carbon steel because of the significant increase of the Ceq, resulting in an easier formation of the quenched martensite structure in the PZ.

Fig. 6 shows the SEM fracture morphologies after the tensile tests for the BM and FSP samples. Obvious necking could be seen on the fracture surface of the BM (Fig. 6(a)), but no obvious area decrease was observed on the fracture surface of the FSP sample that showed a relatively flat fracture characteristic (Fig. 6(b)). Deep dimples could be observed on the fracture surface of the BM, which indicates a ductile fracture (Fig. 6(c)). However, brittle fractured morphology was observed on the fracture surface of the FSP sample with a flat fracture characteristic (Fig. 6(d)). It is clear that brittle fracture occurred during the tensile test of the FSP medium carbon steel. Clearly, subsequent annealing is necessary to increase the ductility and the toughness, which are very important in practical application of the castings.

Both annealed FSP samples (designated as FSP-500 and FSP-600 for annealing at 500 and 600 °C, respectively) still exhibited an ultrafine structure, and much clear morphologies were observed compared to that of the as-FSP state, as shown in Fig. 7. Moreover, lots of carbide particles appeared in both FSP samples after annealing from the detailed SEM microstructure. Besides the carbide particles, many continuous and discontinuous carbide strips could be found in the grains of the FSP-500 sample, which should be attributed to the precipitation of the carbides during the annealing of the martensite [3]. Furthermore, some grains without

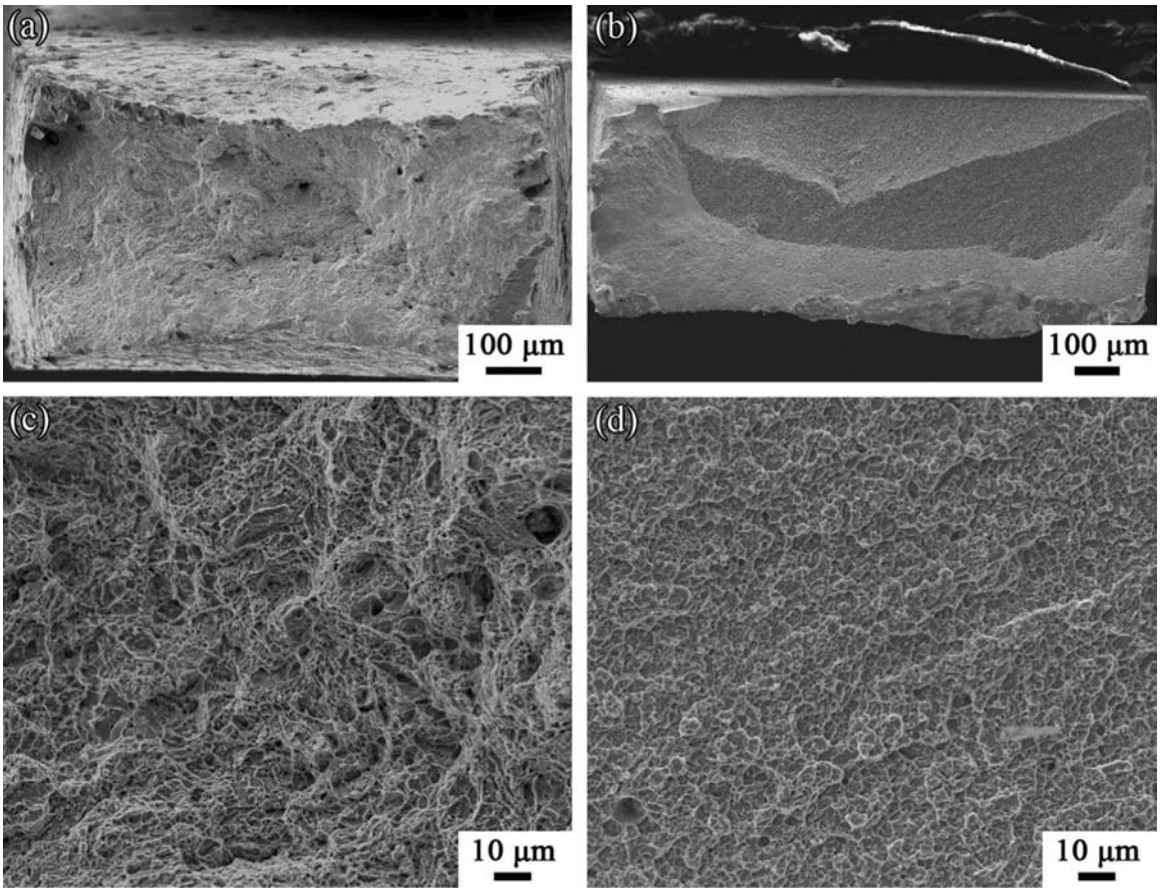

Fig. 6. SEM macrostructure of the fracture surfaces of (a) BM and (b) FSP steel, and microstructure of (c) BM and (d) FSP steel.

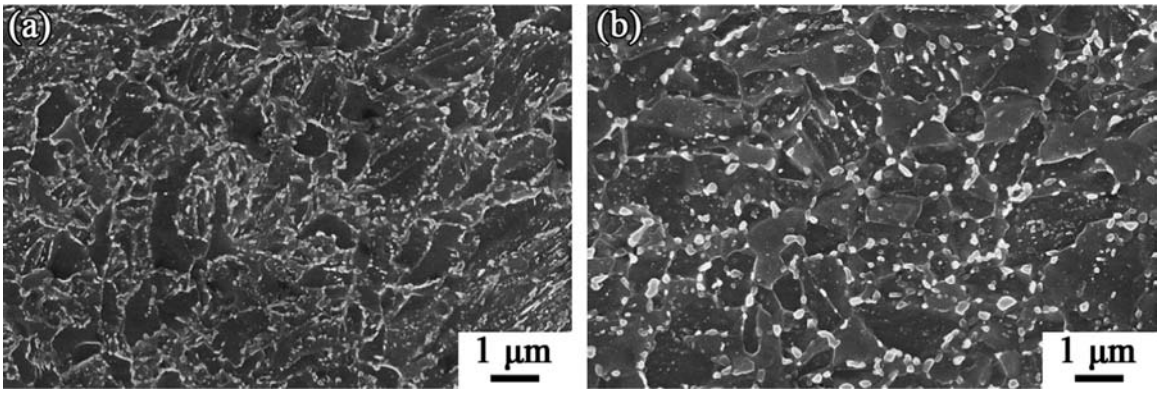

Fig. 7. SEM microstructure of annealed FSP steel: (a) FSP-500 and (b) FSP-600.

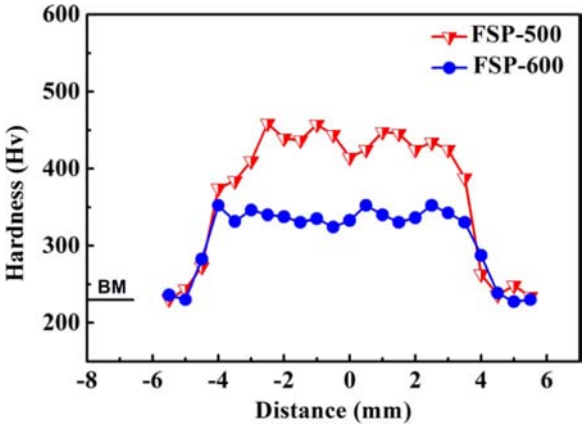

Fig. 8. Hardness distributions of FSP-500 and FSP-600 steels.

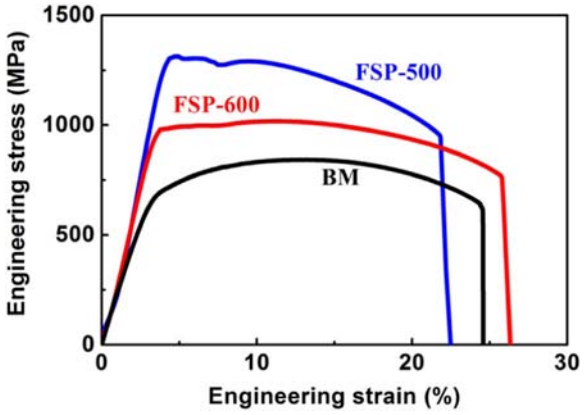

Fig. 9. Engineering stress-strain curves of BM, FSP-500 and FSP-600 steels.

the carbide existed in the FSP-500 sample, indicating that these grains should be the original ferrite grains. However, carbide strips were hardly observed in the grains of the FSP-600 sample, and coarse carbide particles were distributed at the grain boundaries while the fine ones within the grains (Fig. 7(b)).

As indicated above, a dual-phase structure of the ferrite and the martensite was obtained in the as-FSP sample. It is well known that during the phase transformation of the carbon steel, the martensite is transformed from the high temperature austenite, which contains more carbon atoms than the ferrite phase [3]. Therefore, the martainsite phase contained more carbon atoms than the ferrite phase in the FSP steel, due to the insufficient diffusion under rapid cooling rate. After tempering, the carbides precipitated from the martensite phase along the grain boundaries and sub-grain boundaries of the martensite lath. As the tempering temperature and/or time increased, the carbide particles continued to gather and grow from the carbide strips, and gradually diffused to the grain boundaries. Therefore, a large number of the coarse carbide particles were observed at the grain boundaries of the FSP-600 sample, and some fine carbide particles existed in the original martensite phases, as shown in Fig. 7(b).

Fig. 8 shows the hardness distributions of the annealed FSP samples, and the hardness values decreased sharply in the PZs compared to that of the as-FSP state (650 Hv). The hardness value fluctuated in the range of 415–455 Hv in the PZ of the FSP-500 sample, and the average hardness value was calculated to be 438 Hv. More uniform hardness distribution was achieved in the PZ of the FSP-600 samples, which showed a lower average hardness value of 338 Hv.

Fig. 9 shows the typical engineering stress-strain curves of the BM and the annealed FSP samples, and the detailed tensile results are summarized in Table 2. It is clear that the annealed FSP samples still exhibited much higher strength than the BM. The YS and the UTS of the FSP-500 sample were 1270 MPa and 1320 MPa, respectively, which were much higher than those of the BM. Furthermore, the UE of the FSP-500 sample was 5.9%, which reaches the utilizable UE in most industrial applications (~5%). The total elongation of the FSP-500 sample was as large as 18.8%, which was comparable with that of the BM (21.8%). Compared to the FSP-500 sample, the YS decreased to 925 MPa and the UTS to 1020 MPa in the FSP-600 sample, but still higher than those of the BM. Meanwhile, the FSP-600 sample showed a comparable UE of 9.3% to the BM (9.4%), and higher total elongation of 23.4% than that of the BM. Obviously, enhanced mechanical properties with high strength and UE were obtained in the annealed FSP samples.

From the SEM observation of the fracture surfaces of the annealed FSP samples in Fig. 10, it is clear that obvious necking can be observed in the FSP-500 and FSP-600 samples. The original brittle fracture morphologies before annealing transformed to the ductile fracture characteristic after annealing, as shown in Fig. 10 (c) and (d). Dimples could be found on the fracture surfaces of the FSP-500 sample, and more obvious dimples were observed on the fracture surfaces of the FSP-600 sample.

Obviously, enhanced strength-ductility synergy was obtained in the FSP medium carbon steel after annealing, due to the precipitation of the carbides in the martensite phase. Moreover, the present results demonstrate that the desired strength can be achieved by simple annealing process at different temperatures and/or times. Considering the large processed depth and significantly enhanced mechanical properties in the PZ of the FSP medium steel, this study evidently provides an effective surface processing method for the carbon steel castings. More importantly, it can be extended to other materials due to the universality of FSP, especially for the local repair and strengthening.

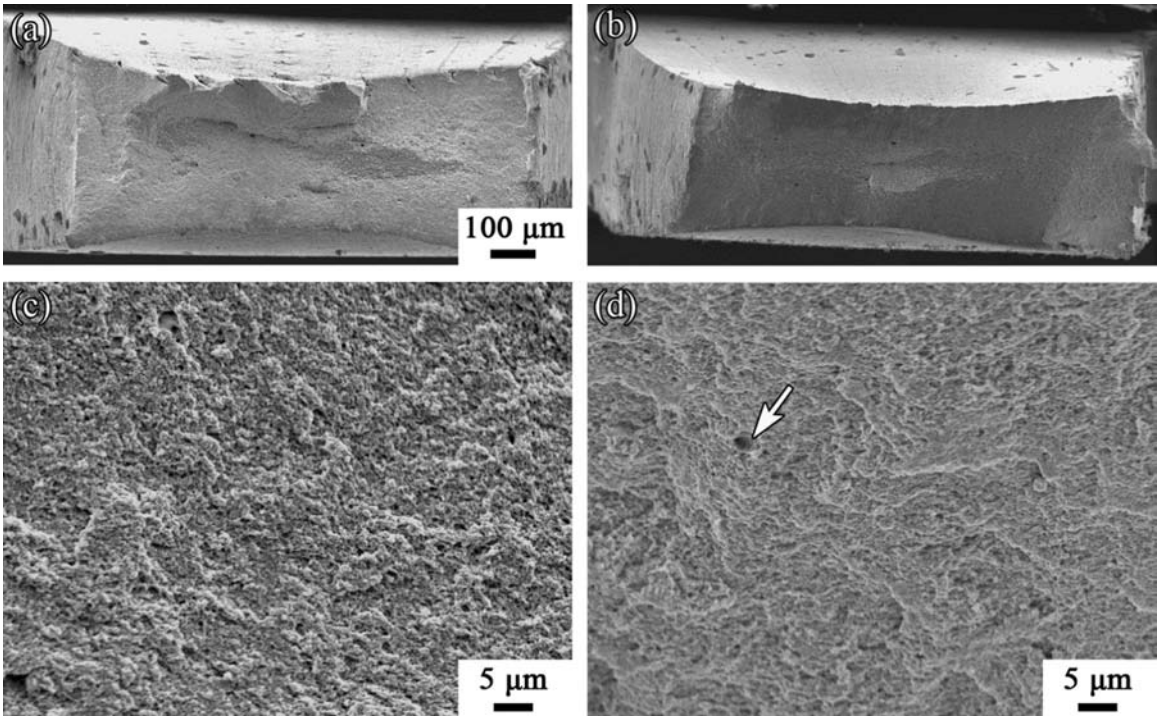

Fig. 10. SEM macrostructure of the fracture surfaces of (a) FSP-500 and (b) FSP-600, and microstructure of (c) FSP-500 and (d) FSP-600.

4. Conclusions

In summary, the following conclusions are reached:

1. Medium carbon steel was successfully friction stir processed at a tool rotation rate of 400 rpm and a traverse speed of 50 mm min^{-1} with additional rapid water cooling, and an obvious PZ with a depth of about 1.5 mm was obtained. The FSP steel was characterized by ultrafine dual-phase structure of the ferrite and the martensite, which exhibited quenched state.
2. Significantly enhanced hardness and the strength were achieved in the PZ compared to the BM. The hardness value of the FSP steel increased to 650 Hv, which was much higher than that of the BM (240 Hv). Very high YS of 2070 MPa was obtained in the FSP steel compared to that of the BM (590 MPa), but the UE was reduced to only 3.0%.
3. After annealing, carbide particles precipitated from the martensite phase, and enhanced strength-ductility synergy was obtained in the FSP steel. Though the YS reduced to 1270 MPa and 925 MPa respectively in the FSP-500 and FSP-600 samples, obviously enhanced ductility was obtained after annealing. Compared to the BM, similar UE of 9.3% and even larger total elongation of 23.4% was achieved in the FSP-600 sample.

Acknowledgments

This work was supported by the National Natural Science Foundation of China under grant Nos. 51301178, 51331008, and 51201163.

References

[1] H. Berns, W. Theisen, Ferrous Materials, Springer, Leipzig, 2008.
[2] H. Sun, L. Li, X. Cheng, W. Qiu, Z. Liu, L. Zeng, Iron Mak. Steel Mak. 42 (2015) 439–449.
[3] H.K.D.H. Bhadeshia, R.W.K. Honeycombe, Steels Microstructure and Properties, Third ed., Butterworth-Heinemann, Elsevier Ltd, Oxford, 2006.
[4] J. Sakamoto, Y.S. Lee, S.K. Cheong, J. Mech. Sci. Technol. 28 (2014) 3555–3560.
[5] Y. Harada, H. Kosaka, M. Ishihara, Steel Res. Int. 84 (2013) 1333–1339.
[6] K. Lu, J. Lu, Mater. Sci. Eng. A 375 (2004) 38–45.
[7] H.W. Huang, Z.B. Wang, J. Lu, K. Lu, Acta Mater. 87 (2015) 150–160.
[8] R.S. Mishra, Z.Y. Ma, Mater. Sci. Eng. R 50 (2005) 1–78.
[9] Z.Y. Ma, Metall. Mater. Trans. A 39 (2008) 642–658.
[10] R. Nandan, T. DebRoy, H.K.D.H. Bhadeshia, Prog. Mater. Sci. 53 (2008) 980–1023.
[11] M. Hajian, A. Abdollah-zadeh, S.S. Rezaei-Nejad, H. Assadi, S.M.M. Hadavi, K. Chung, M. Shokouhimehr, Appl. Surf. Sci. 308 (2014) 184–192.
[12] K. Ito, T. Okuda, R. Ueji, H. Fujii, C. Shiga, Mater. Des. 61 (2014) 275–280.
[13] A. Rahbar-kelishami, A. Abdollah-zadeh, M.M. Hadavi, R.A. Seraj, A.P. Gerlich, Appl. Surf. Sci. 316 (2014) 501–507.
[14] T. Nagaoka, Y. Kimoto, H. Watanabe, M. Fukusumi, Y. Morisada, H. Fujii, Mater. Des. 83 (2015) 224–229.
[15] P. Xue, Z.Y. Ma, Y. Komizo, H. Fujii, Mater. Lett. 162 (2016) 161–164.
[16] C.I. Chang, X.H. Du, J.C. Huang, Scr. Mater. 57 (2007) 209–212.
[17] P. Xue, B.L. Xiao, Z.Y. Ma, Acta Metall. Sin. 50 (2014) 245–251.
[18] J.Q. Su, T.W. Nelson, C.J. Sterling, Scr. Mater. 52 (2005) 135–140.
[19] P. Xue, B.L. Xiao, Z.Y. Ma, J. Mater. Sci. Technol. 29 (2013) 1111–1115.
[20] P. Xue, B.L. Xiao, W.G. Wang, Q. Zhang, D. Wang, Q.Z. Wang, Z.Y. Ma, Mater. Sci. Eng. A 575 (2013) 30–34.
[21] H.K.D.H. Bhadeshia, T. DebRoy, Sci. Technol. Weld. Join. 14 (2009) 193–196.
[22] R. Rai, A. De, H.K.D.H. Bhadeshia, T. DebRoy, Sci. Technol. Weld. Join. 16 (2011) 325–342.
[23] M. Bruneau, C.M. Uang, A. Whittaker, Ductile Design of Steel Structures, Mcgraw-Hill, New York, 1998.
[24] P. Xue, B.L. Xiao, Q. Zhang, Z.Y. Ma, Scr. Mater. 64 (2011) 1051–1054.